Photochromic behavior of ZnO/MoO3 interfaces.

Ines Andron, Léa Marichez, Veronique Jubera, Christine Labrugère, Mathieu Duttine, Christine Frayret, Manuel Gaudon

Photochromic behavior of ZnO / MoO_3 interfaces.

Ines Andron,†, ‡ Léa Marichez, † Véronique Jubera, † Christine Labrugère, † Mathieu Duttine, † Christine Frayret, ‡ Manuel Gaudon†,*.

† CNRS, Univ. Bordeaux, Bordeaux INP, ICMCB, UMR 5026, F-33600 Pessac, France

‡ Laboratoire de Réactivité et de Chimie des Solides (LRCS), CNRS UMR 7314, Université de Picardie Jules Verne, 80039 Amiens, France

KEYWORDS Photochromism ; Schottky barrier ; Interfaces ; Photo-redox, Zinc oxide ; Molybdenum oxide.

ABSTRACT: ZnO / MoO_3 powder mixture exhibits a huge photochromic effect in comparison with the corresponding single oxides. The coloring efficiency of such combined material after UV-light irradiation was studied in terms of intensity, kinetics, as well as ZnO / MoO_3 powder ratio. Additionally, the incidence of the pre-treatment step of the ZnO and MoO_3 powders under different atmospheres (air, Ar or Ar/H_2 flow) was analyzed. The huge photochromic effect discovered herein was interpreted as the creation of "self-closed Schottky barrier" at the solid/solid interfaces between the two oxides, associated with the full redox reaction which can be pictured by the equation: $ZnO_{1-\varepsilon}$ + MoO_3 → ZnO + $MoO_{3-\varepsilon}$. Remarkable optical contrast between virgin and color states as well as self-bleaching in dark allowing the reversibility of the photochromism are emphasized. From this first discovery, deeper characterization of the self-bleaching process shows that the photochromic mechanism is complex with a bleaching efficiency (possibility to come back to the virgin material optical properties without any deterioration) and a bleaching kinetics, which are both depending on the coloring irradiation time. This demonstrates that the oxygen exchange through the Schottky interface proceeds in at least two convoluted steps: an anionic surface exchange allowing a reversibility of the redox reaction followed by bulk diffusion of the exchanged anions which are then definitively trapped. An emergent "negative photochromism effect", (i.e. photochromism associated with a self-bleaching instead of a darkening under irradiation), is observed after long irradiation time.

Introduction.

Photochromic displays are considered as one of the most promising solutions to enhance light control and to reduce energy consumption in buildings when coated as thin films on smart windows[1-3]. Inorganic photochromic compounds, which exhibit a good stability and cost efficiency in comparison with their organic counterparts (*e.g.* azobenzene, diarylethene or spiropyran)[4-6], exhibit a photochromic mechanism typically based on the photo-reducibility of the metallic element in wide band gap semiconductors as MoO_3[7-10], WO_3[7,11-15], TiO_2[16-17], V_2O_5[18], or Nb_2O_5[19]. Accordingly, visible and infrared light through windows can so be tuned depending on the light irradiation intensity thanks to the redox reaction allowing the transition between bleached and coloured states. Besides, such key application, needing some large-scale production and transparent thin films feasibility, bistable photochromic compounds can also find applications such as electronic shelf labels, electronic tag, chemical sensors or optical data storage media. Discovered by Deb *et al*,[20], WO_3 is largely the most studied candidate among the inorganic photochromic materials. It exhibits the best photochromic efficiency (*i.e.* optimal optical contrast between bleached and coloured states). Two recent reviews from Jiang *et al*[2] and Yao *et al*[21] declined however the various advances performed on WO_3-based photochromic materials. These works pose the strongest limitation of such photochromism: none or poor reversibility, the recovering of the bleached state being accessible only from oxidative treatments (*i.e.* thermal or chemical). Furthermore, the photochromic efficiency of inorganic oxides can be increased using different strategies, especially by a combination of these compounds with other organic or inorganic materials. This leads indeed to the creation of solid-solid interfaces described as Schottky barriers, which help the charge depletion (*i.e.* spatial separation of the holes and the electrons created by irradiation) and thus promotes photo-redox reactions. In this kind of materials, it has been observed through numerous studies performed by Yao *et al*[22-25] that MoO_3 used alone does not exhibit any satisfying photochromic contrast whereas its combination with gold or platinum nanoparticles to form Schottky barriers leads to a drastic improve-

ment of the photochromic abilities. This effect is especially evidenced in terms of solar transmittance contrast through thin composite films between bleached and colour states and through an extension of the light response from ultraviolet (UV) light to visible light or solar radiation. The enhancement in the visible-light photochromism for MoO_3 / Au or MoO_3 / Pt thin-film samples is explained from the capture by Au and Pt resulting in a longer electron – hole pair separation lifetime, per analogy with the photocatalytic enhancement effect when Pt or Au metal is deposited on inorganic semiconductor surfaces[26-27]. In parallel, Ramirez-Bon *et al*[28] have shown that the generation of colour centres in MoO_3 thin films under UV-light absorption is more effective when MoO_3 layers are coated on CdS glass substrates. This phenomenon is ascribable to the formation of a Schottky barrier at the interface of the two inorganic semi-conductors. In a similar way, the combination of WO_3 and CdS also lead to enhanced photochromic activity, as shown by Zhao *et al*[29]. Such enhancement of MoO_3 or WO_3 photochromism thanks to the combination with another metal-oxide was recently explored by proposing various composite powder / films including for instance: MoO_3-WO_3[30-32], ZnO-WO_3[33-34], TiO_2-WO_3[35-36], TiO_2-MoO_3[37-38], etc., or even crystalline-amorphous WO_3-WO_{3-x}[39] particles with abundant proton sources and rich-oxygen vacancies in the homo-junctions.

As a continuation of these works, we examined in this study the exceptional photochromism exhibited by a hetero-junction composite powder prepared from the mechanical mixing into agate mortar of adequate ZnO and MoO_3 commercial samples (provided by Alfa Aesar: CAS-1314-13-2, D03Y023 and CAS-1313-27-5, E01S050). This material was characterized in terms of solar modulation efficiency, photochromic kinetics and reversibility. The photochromic intensity was found to be clearly correlated to the power of the UV-light excitation source, clearly demonstrating that the proposed powder mixture can get an efficient reversible colour switch produced in few minutes under solar irradiation followed with a self-bleaching occurring in few hours in dark conditions. Moreover, the possibility to quench the photochromism effect or to tune the reversible behaviour from oxidative gas treatment has led to reinterpret the redox mechanism initially proposed by Deb *et al*[20], in the sixties, with respect to the non-reversible WO_3 or MoO_3 photochromism owing to the formation of tungsten or molybdenum bronzes. From the proposed mechanism, *i.e.* a self-looped redox reaction through the MoO_3/ZnO interfaces thanks to the opposite exchange of oxygen anions and electrons; we clearly envision that new photochromic smart films can be designed in next future.

Supplementary Figure S1 schematically illustrates the proposed photochromic mechanism on ZnO / MoO_3 solid /solid interfaces. It is composed of the following steps : (a) owing to the similar band gap energy (E_g) of about 3.2-3.3 eV for the two wide band gap oxides, the combination of the two oxides allows the formation of a Schottky barrier associated with the injection of the electrons due to exciton pairs formation from the conduction band (CB) of the ZnO to the CB of the MoO_3, the injected electrons into this latter thus causing the reduction of Mo^{6+} ions into Mo^{5+} ones, (b) then the intervalence charge transfer (IVCT) takes place between two consecutive Mo^{6+} and Mo^{5+} ions along oxo-bridges, (c) finally, the IVCT results in a deep blue coloration being associated with an absorption band located at the frontier between infrared and visible domains with an intensity increasing *vs.* the Mo^{5+} density. To end the redox process, the charge depletion taking place at the interface has to be compensated. It was proposed earlier by Deb *et al*[20] that the ZnO valence band (VB) holes (h^+) recombination could be ensured by water molecules oxidation in link with the formation of molybdenum bronzes (H_xMoO_3). However, this mechanism still remains a point of controversies.

Experimental.

The compound structures were characterized by X-ray diffraction analysis (PANanalytical X'Pert Pro instrument Cu $K_{\alpha 1}$ = 1.54056 Å, $K_{\alpha 2}$ = 1.54439 Å and 2θ range from 8° to 80°).

The morphology of the as-prepared particles was observed by scanning electron microscopy (SEM) using JEOL JSM-6700F.

Electron Paramagnetic Resonance (EPR) experiments were performed from room temperature down to 4.2 K with a Bruker ESP300E spectrometer equipped with a rectangular TE104 cavity and an Oxford ESR910 liquid helium cryostat. The main spectroscopic parameters are as follows: microwave frequency 9.54 GHz and power 10 mW, magnetic field modulation frequency 100 kHz and amplitude 0.5 mT, spectral resolution 0.3 mT/pt and sweep time 82 ms/pt. WinEPR and WinSIMFONIA softwares were used to analyze the EPR spectra and simulate the detected signals. DPPH was used as external reference to calibrate the spectrometer.

X-ray photoelectron spectroscopy (XPS) was performed using a photo-electron spectrometer (ThermoScientific K-Alpha) with a monochromatic Al K_α X-ray source (1486.6 eV). Relative element concentrations were determined by the integral areas of the core-level spectra, the spectra were fitted into several peaks using a convolution of Gaussian and Lorentzian functions.

Fourier Transform Infrared Spectra were recorded using a BRUKER Equinox 55 FTIR spectrometer with a spectral resolution of 4 cm^{-1}. The recording and storage of a spectrum was performed from 400 to 4000 cm^{-1}. The diffuse reflectance mode measurements were conducted using a Specac selector diffuse reflection cell. Sample to be analyzed were prepared by spreading crushed powders (3 wt%) in anhydrous (spectroscopy grade) KBr on Cronical support.

Diffuse reflectance spectra were recorded at room temperature from 200 to 2500 nm on a Cary 5000 spectrophotometer using an integration sphere (spectral resolution: 1 nm and band length: 2 nm). Halon was used as white reference. RGB space colorimetric parameters were determined from the spectra using a two-step mathematic treatment. The first step consists in extracting the XYZ tristimulus values (defined by the CIE, 1964) from the integration (over the visible range, i.e. from λ = 380 nm up to 780 nm) of the product of x(λ), y(λ) or z(λ) functions (CIE – 1964) with the diffuse reflectance, such $X=\int x(\lambda).R(\lambda)d\lambda$.

Irradiations were performed using a UV Hg-lamp (Vilbert Lourmat 8.LC) at a monochromatic wavelength of 365 nm. The sample is placed at 10 cm from 8 W tubes.

Results and discussion.

The evolution of the reflectance as a function of UV-light irradiation time for the single ZnO and MoO_3 powders (presented in Figure S2 along with SEM micrographs of the ZnO and MoO_3 raw oxides) indicates that such oxides when they are apart exhibit negligible photochromic effect. In SEM micrographs (Fig.1) showing the morphology of ZnO / MoO_3 powder mixture (50 / 50 wt%) prepared from mechanical grinding in agate mortar, we observe that ZnO micron particles are dispersed on MoO_3 platelet surfaces, leading to large solid / solid interface areas (see Figures S3 and S4 for comparison of the photochromic efficiency of different ZnO/MoO_3 weight ratios or from gravitational mixing process). The powder mixture was exposed to low-power UV-light irradiation in such a way that the power per surface unit received by the sample is equal to 5.6 W/m^2, *i.e.* a value close to the UV-daylight irradiance received in London, in September[40]. The reflectance (R%) of the material *vs.* UV-light irradiation time on 400-2500 nm wavelength range is recorded and can be transformed in Kubelka-Munk ($K/S = (1-R\%/100)/(2\times R\%/100)^2$) absorbance spectra. K/S transforms exhibit an intensity of the absorption phenomena proportional to the chromophore concentration and are so used for kinetic analysis.

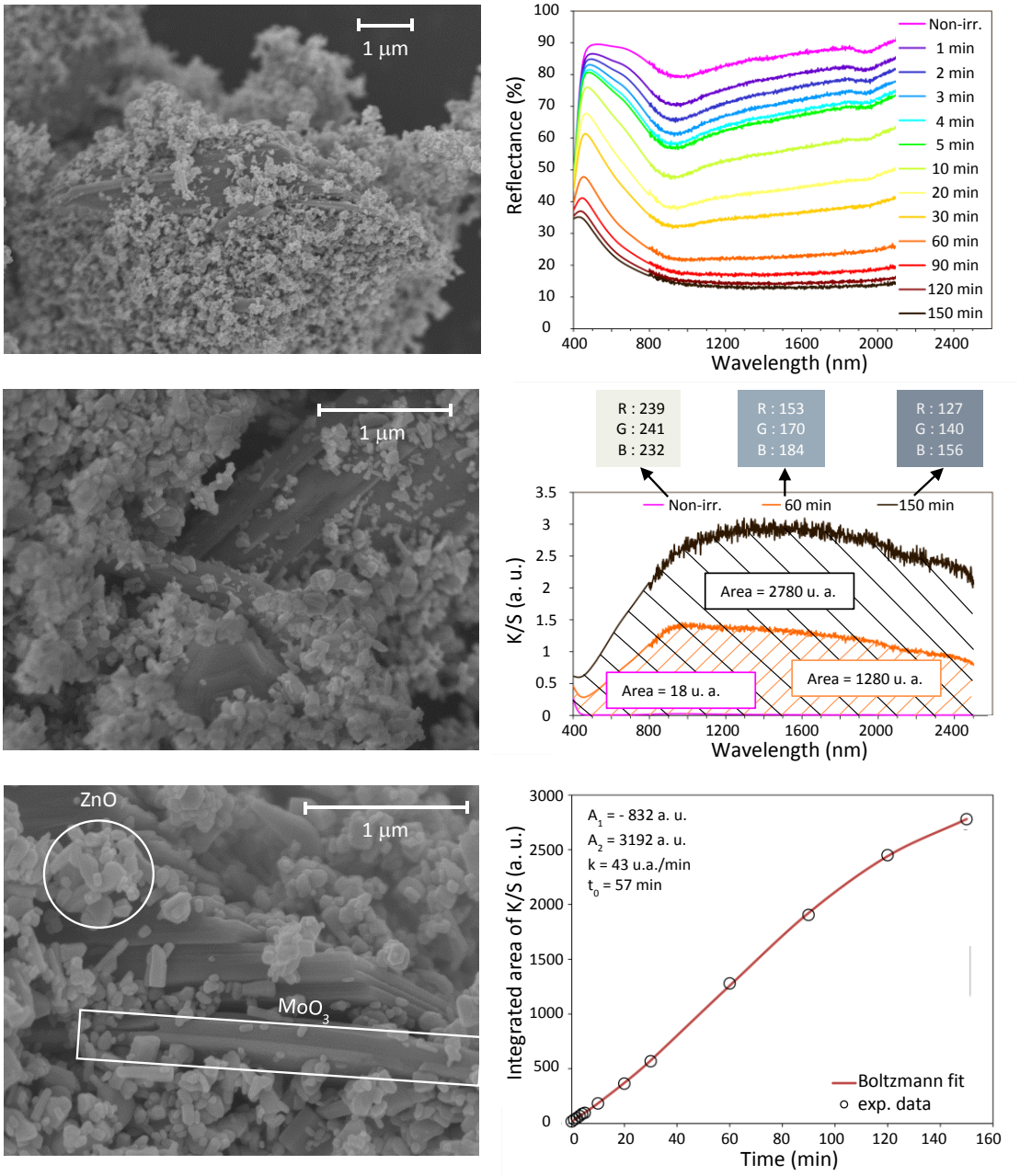

Fig. 1: Left: SEM pictures of the ZnO/MoO_3 mixture at different scales; Right: i) top: evolution of the mixture reflectance spectra *vs.* UV-light excitation time, ii) middle: corresponding colors and K/S Kubelka-Munk transforms for three characteristic irradiation times and iii) bottom: evolution of the total K/S absorbance (400-2500 nm) *vs.* irradiation time and picture of the laboratory logo thanks to a paper mask to limit the irradiation area.

The powder mixture coloring efficiency is really exceptional in comparison with the two single oxides which are associated, with intermediate blue color already obtained after 60 min. of irradiation. The associated kinetics can be fitted considering a sigmoid (S curve): $K/S = A_1+(A_2-A_1)/(1+\exp(t_0-t/k))$, with t and k in min representing the time on S inflexion point and the inflexion point slope, respectively, while A_1 and A_2 correspond to the onset and ending asymptotic values. In these conditions, the characteristic time (k) is close to 1 hour.

Hence, in the as-prepared powder mixture, the surface which possesses oxygen deficiency should be attributed to the ZnO one, in good agreement with the intrinsic n-types properties of the zinc oxide (which can be written as $Zn_{1+\varepsilon}O$ chemical composition with segregation of the anionic vacancy at the surface as shown in our own previous works[41-42]). This naturally oxygen-deficient surface plays a crucial role as reducer in the induced photo-redox process, and the air atmosphere pre-treatment kills the photo-

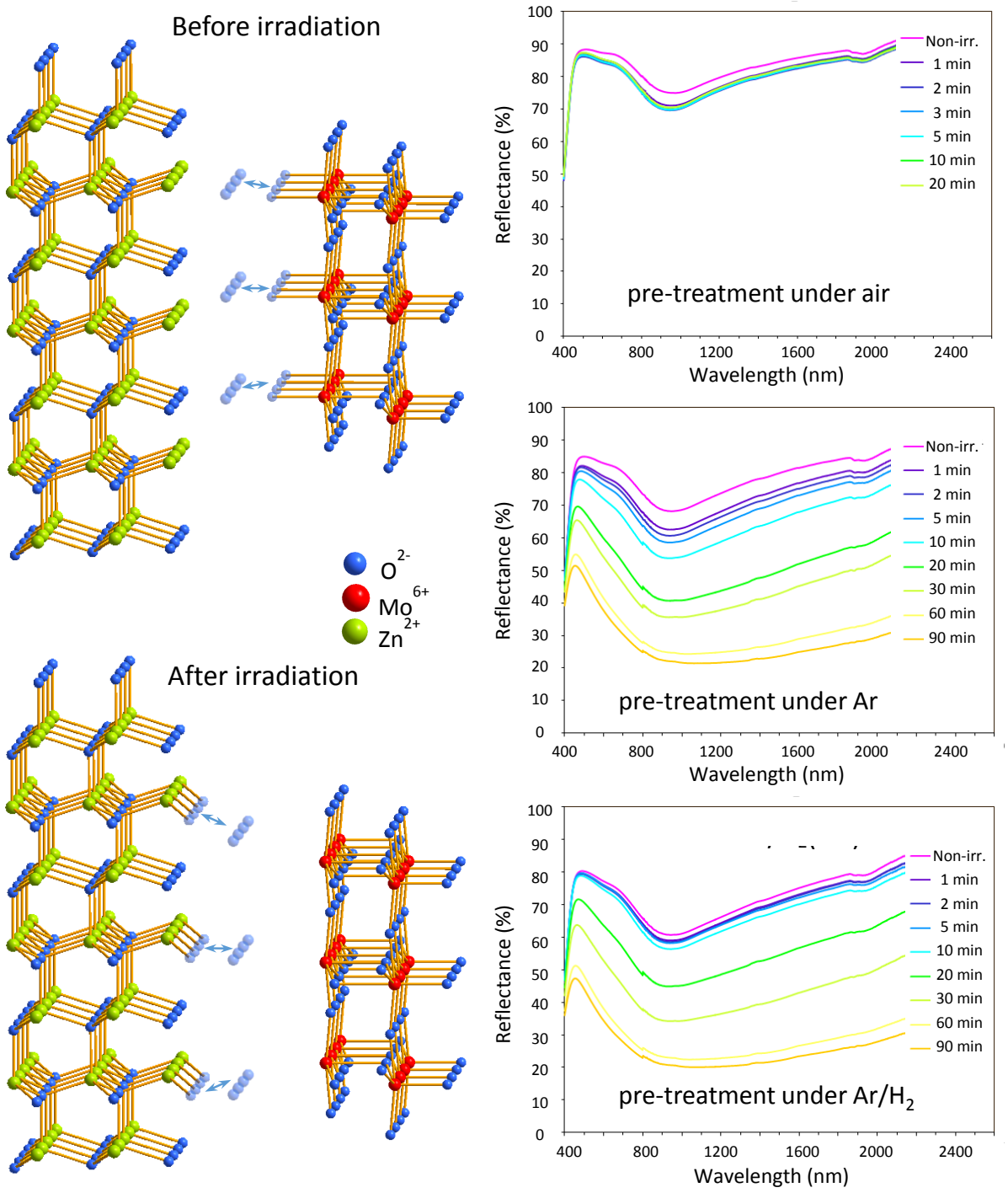

Fig. 2: Left: Oxygen exchange representation at the ZnO/MoO_3 interface (the two crystalline structures are plotted with the same sale factor); Right: evolution of the mixture reflectance spectra as a function of UV-light excitation time, after respectively, air, Ar or Ar/H_2 pre-treatment (from top to bottom).

-chromic effect without any doubt due to a pre-oxidation of the ZnO oxide surface. This result also indicates that ZnO acts not only as an electron donor after the exciton creation thanks to UV-light irradiation, but also as an oxygen anion recipient in order to "loop" the complete redox equation occurring on the Schottky barrier: $ZnO_{1-\varepsilon} + MoO_3 \rightarrow ZnO + MoO_{3-\varepsilon}$. The ability of MoO_3 surfaces to be easily peeled off from their oxygen anions let this oxide act like an oxygen source and it is obviously the reason why the photo-redox mechanism at ZnO/MoO_3 interface is working so well. Furthermore, the good spatial agreement between the oxygen-oxygen distances on MoO_3 surfaces (local oxidizer species) and the zinc-zinc distance on ZnO surfaces (local fuel species) (as exemplified in Fig. 2, on which the two oxides are drawn with same scale bar) could allow the oxygen exchange between the two solids and thus account for the exceptional photochromic effect exhibited by the ZnO/MoO_3 interfaces.

This proposition of a photo-redox mechanism occurring without the intervention of water molecules is strongly reinforced by infrared studies (before and after irradiation, Figure S5) indicating the lack of band intensity increase for the O-H group bending vibration upon irradiation. By a comparison with the X-ray diffraction pattern of a virgin mixture, a prolonged irradiation (1.5 hours) leads to the appearance of new diffraction peaks neighboring the main ones relative to MoO_3 (Figure S6). This effect can be associated with a clear modification of the MoO_3 bond lengths of some crystallites. Most probably, this local modification should concern the MoO_3 crystallites in direct contact with ZnO oxide. This is a consequence of the reduction of a significant part of the Mo^{6+} ions into Mo^{5+} anions after UV-light excitation. EPR spectra (Figure S7) on powder mixture, which is either non-irradiated or irradiated during 15 and 180 min clearly indicate the detection of a new signal corresponding to Mo^{5+} species induced through irradiation. At last but not least, the XPS studies have confirmed the increase of the Mo^{5+} quantity comparing the non-irradiated, the 15 and the 180 min irradiated samples. Indeed, as shown on Mo *3d* spectra (Figure S8), in good agreement with EPR observations, the Mo^{5+} proportion in each sample are equal to 0 %, 3.4 mol%, 5.2 mol% and 15.5 mol% respectively for the pure MoO_3 as reference, non-irradiated ZnO-MoO_3 mixture, 15 min irradiated mixture and 2 hours irradiated mixture (the composition of Mo oxidation states was estimated by the deconvolution of Mo *3d* doublet and relative element concentrations were determined by the integral areas of the core-level spectra.) Interestingly, the XPS spectra of O *1s* region of same mixtures and in regard of the ZnO and MoO_3 samples as references show that the O *1s* core-level spectrum exhibits three different forms of oxygen. Basing on literature,[42-44] the peak located at lower energy about 530.5e V belongs to the Zn–O bonding in ZnO Würtzite structure ; peaks located at 531.7 and 532.6 eV can be respectively ascribed to the Zn–O surface bonding and to the presence of C–O bonding originated from the oxy-carbonated molecules adsorbed on the ZnO surface. It appears that in both pure MoO_3 and ZnO samples the intermediate signal is absent or weaker than in the Zno-MoO_3 mixtures (equal to about 18 % whatever the irradiated time). Hence, the mechanical grinding of the ZnO and MoO_3 powders seems well at the origin of the engagement of new surface oxygens on the ZnO compound. XPS studies strongly reinforce our hypothesis of the creation of dangling bonds between the oxygen from the MoO_3 surface and the Zn^{2+} cations available on the ZnO oxide surface, this creation allowing then the capacity of an exchange of electrons from the two oxides while a photo-irradiation is applied.

The photochromic reversibility studies of MoO_3 or WO_3 oxide compounds combined or not with metallic nanoparticles or another metal oxide show poor reversibility with no additional help. Several solutions have been tested to accelerate the bleaching rate, such as the addition of an oxidizer (ozone, water peroxide, etc.[15,45-47]). However, a direct issue is a strong limitation for the targeted applications. It can be noted that a fast-self-bleaching phenomenon was recently reported on the photochromic response of WO_3 oxides[39], the term fast self-bleaching being used for a process taking 8 hours. Fig. 3 shows that a self-bleaching process is observed on the as-prepared ZnO/MoO_3 (50/50) mixture previously irradiated with different UV exposure times: from 5 min. up to a time allowing the saturation of the coloring rate (6 hours irradiation).

Kinetics and efficiency studies of the self-bleaching process were then undertaken on these different samples (Fig. 3 and Figure S9). After 5 min. of irradiation leading to weak coloration intensity, the bleaching process is rapid and nearly 100% efficient: a bleached state with whiteness near to the virgin state is recovered after 8 hours in dark. After 10 min. of irradiation, the bleaching process is already deteriorated, the recovery speed slows down and the efficiency amount only to 85% (i.e. the asymptotic values reached after prolonged self-bleaching time of the normalized K/S integrated intensity is about 15%). This deterioration is strongly reinforced after 1 hour of irradiation: bleaching rate is decreased to about 50%, the bleaching time being very long. Indeed, half the way back to the transmittance of the virgin material is only reached after few days in dark. However, it can be noticed that the bleaching can be also produced by the addition of water peroxide (the bleaching is almost immediate), but in this latter case, the next photochromic activities are definitively quenched (Figure S10). At last but not least, after 4 hours of irradiation, the bleaching process is definitely quenched, even, in dark, the coloring of the ZnO : MoO_3 mixture is prolonged: a "negative photochromic effect" is so observed ("negative photochromism" in the sense that a bleaching phenomenon under irradiation follows the coloring effect for long UV exposure).

Therefore, a cycling test involving 10 min. of irradiation followed by 11h50 min in dark (12 hours for a full cycle), which was shown to correspond to a good compromise, in first approximation, equivalent coloring and bleaching rates, was repeated several times on the ZnO/MoO_3 powder mixture (Fig. 4). With such cycling, the average absorption (integrated area of K/Spectra on 400 – 2500 nm) is still constant versus the number of cycles, whereas the optical contrast between colored and bleached states (which can be defined by the pondered sum of the deviations between the R, G and B colorimetric parameters of the colored and bleached states) is progressively damped and tend to zero after 5 cycles.

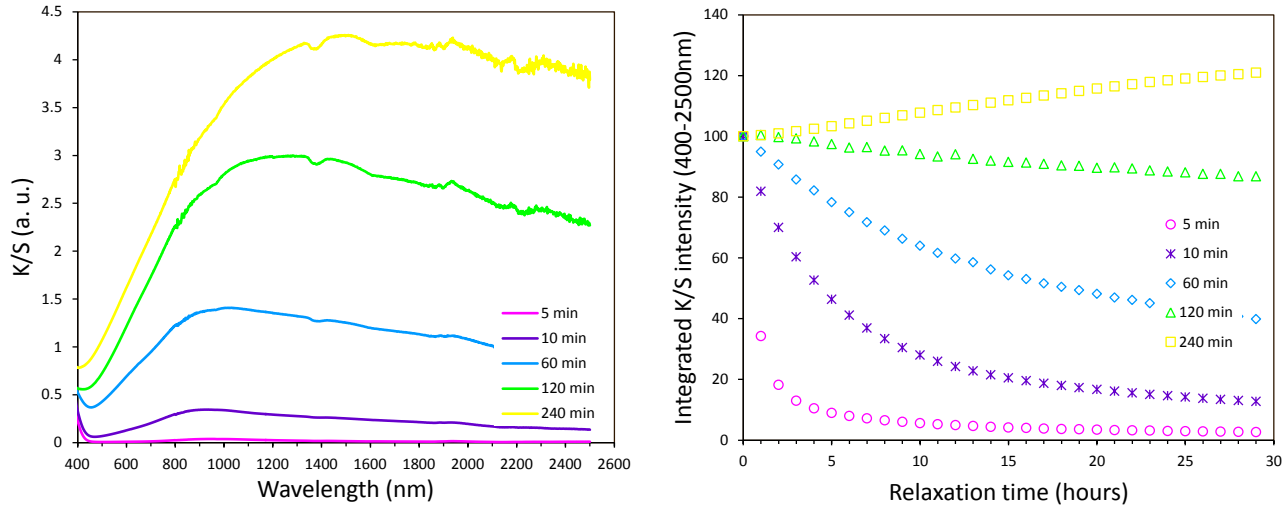

Fig. 3: Left: K/S Kubelka-Munk transforms of the ZnO/ MoO_3 powder mixtures after different irradiation times and their normalized self-bleaching properties; Right: evolution of the K/S total absorbance (400-2500nm) versus time (under dark).

In detail, at the exception of the 1st cycle, showing a behavior which seems to emphasize a necessary initiation of the photochromic phenomenon (the reached color state is less deep than the ones of the other cycles), the loss of the photochromic response is due to both the decrease of the coloring and the bleaching rates versus cycling, leading after few cycles to a stable intermediate coloration between the initial virgin state and the 1st cycle color state. This observation linked to a fatigue resistance was already observed on organic photochromic compounds (diarylethenes[48]) in which the colorless ring-opened states and the colored ring-closed states are submitted to interconversion at different wavelengths. A second cycling test performed this time through 1 hour of irradiation followed by only 11h bleaching, *i.e.* with a coloring rate higher than the bleaching rate on each cycle, also demonstrates the damping of the photochromic effect but superimposed with a progressive coloring trend. Herein, the fatigue of the photochromic cycling can be explained, in regard of the fast kinetic of the coloring half cycle in comparison with the low kinetics of the bleaching half cycle as well from cycling conditions not allowing 100% coloring as well as 100% bleaching rates.

In a more applicative view, these experiments show that further improvements must be done in order to achieve a functional photochromic material able to maintain a sufficient and robust optical contrast between bleached and color states versus cycling. The fatigue could come from a combination of (i) the saturation through cycles of ZnO surfaces from oxygen anions given by the MoO_3 surfaces, very long times being necessary to fully refresh the ZnO surfaces from supernumerary anions, (ii) the too high stability of some oxygen anions given by the MoO_3 oxides to the ZnO oxide, leading to too much stable covalently-bonded oxygen anions on ZnO surfaces, or (iii) the bond valence hole diffusion (anionic vacancies diffusion) into the MoO_3 bulk structure (as revealed from X-ray diffraction on the powder mixture obtained after very long irradiation time). We definitively consider that this last hypothesis is the good one since it is coherent with the photochromic effect evolution under cycling and our schematic redox mechanism. Under light-excitation, the MoO_3 oxide (oxidizer) gives surface anions oxygen to the ZnO oxide (reducer) due to charge carrier transfer from CB in the reverse way from ZnO to MoO_3 compound. In dark, the missing oxygen anions at the MoO_3 surface can then be replaced by two types of oxygens: the ZnO surface oxygen atoms which were previously transferred from MoO_3 in the coloring half cycle (ensuring the reversibility of the photochromic effect: self-bleaching) and the oxygen atoms arising from the diffusion from the MoO_3 bulk to the MoO_3 surface. Unfortunately, this second oxygen path definitively stabilizes the reduction of the MoO_3 oxide and a blue coloration occurs.

Furthermore, by filling cationic receptor and so preventing the return of some oxygen anions previously transferred to ZnO surface, this phenomenon also blocks some oxygen anions on the ZnO surface, thus stopping further oxygen exchanges between ZnO and MoO_3. The oxygen vacancies reorganization with diffusion from the MoO_3 surface to the bulk crystalline structure could explain the negative photochromic effect observed after prolonged irradiation; indeed, the hole diffusion is associated to a desegregation of the Mo^{5+} cations from surface and tends to favor the probability of the $Mo^{5+} \rightarrow O^{2-} \rightarrow Mo^{5+}$ intervalence charge transfer. Anyway, the next development should concentrate to limit the oxygen exchanges necessary to "loop" the redox reaction at the Schottky interface between these two oxides to the material surface, and, to maintain high optical contrast in order to avoid the possibility of hole diffusion into the MoO_3 bulk. Concerning material design of the MoO_3 oxide, the synthesis of very thin lamellar platelets could for instance be the solution for future developments.

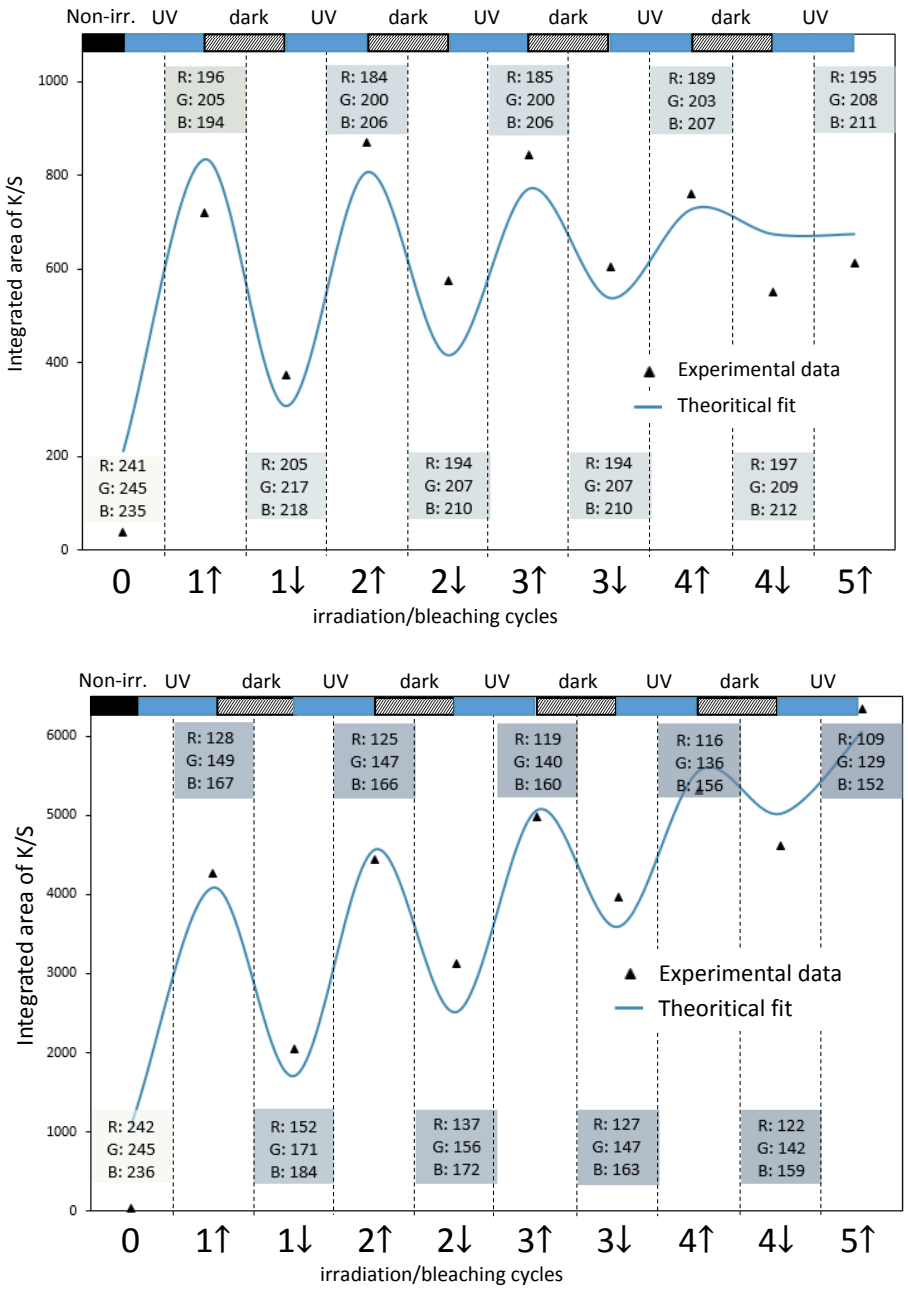

Fig. 4: Photochromic effect cycling tests with two different cycling parameters: Top: 10 min. irradiation / 11h50 min. in dark; Bottom: 1 hour irradiation / 11 hours in dark.

Conclusion.

In this study, it has been shown that ZnO / MoO_3 powder mixture exhibits a huge photochromic effect, even under low power UV-irradiation, due to the creation of "self-closed Schottky barrier" at the solid/solid interfaces. Despite a materials combination made by rough mechanical grinding, XPS studies revealed that oxygen bridging bond at the ZnO-MoO_3 interfaces are formed, creating the Schottky interface. Pre-annealing on the ZnO powder under different atmospheres has evidenced that the ZnO surface must be oxygen-deficient to act like an efficient reducer of the MoO_3 compound and allow Schottky barrier creation. Such combined material shows an exceptional coloring efficiency in terms of intensity, but also shows reversibility: bleaching under dark condition, opening a potential break-through in the use of inorganic photochromic material. Next studies will focus on acting on the parameters making able to tune this complex photochromism in intensity, cyclability and coloring/bleaching speeds (as, for illustration, varying the ZnO and MoO_3 morphologies and surface chemistry using soft-chemistry synthesis routes, by doping the ZnO with M^{3+} cation in order to inject more electrons in the ZnO conduction band for hence favoring the photo-redox mechanism, by tuning the band gap of both oxides for reaching an ideal matching, etc.)

ASSOCIATED CONTENT

Supporting Information.

Supporting information includes only supplementary Figures, reported as supplementary Figure Sx. Supplementary Figure S0 is an introduction scheme of the photochromism mechanism; supplementary Figures S1a, S1b and S1c are extended content associated to Fig. 1; in a same way, supplementary Figures S2a, S2b, S2c and S2d are extended content of Fig. 2 and supplementary Figure S3a and Figure S3b are extension of Fig. 3.

This material is available free of charge via the Internet at http://pubs.acs.org." For instructions on what should be included in the Supporting Information as well as how to prepare this material for publication, refer to the journal's Instructions for Authors.

AUTHOR INFORMATION

Corresponding Author

*Corresponding authors: manuel.gaudon@icmcb.cnrs.fr

Author Contributions

The manuscript was written through contributions of all authors. All authors have given approval to the final version of the manuscript. All authors contributed equally.

Funding Sources

The authors thank the CNRS, the Nouvelle Aquitaine region. This study was carried out with financial support from the French State, managed by the French National Research Agency (ANR) in the frame of program PRIDE (n° ANR-16-CE08-0029).

REFERENCES

1. Qi, W.; Li H.L.; Wu, X. Stable Photochromism and Controllable Reduction Properties of Surfactant-Encapsulated Polyoxometalate/Silica Hybrid Films, J. Phys. Chem. B, 2008, 112, 8257-8263

2. Wang, S.; Fan, W.; Liu, Z.; Yu A.; Jiang, X. Advances on Tungsten Oxide Based Photochromic Materials: Strategies to Improve their Photochromic Properties, J. Mater. Chem. C, 2018, 6, 191-212

3. Granqvist, C.G. Electrochromics for Smart Windows: Oxide-Based Thin Films and Devices, Thin Solid Films, 2014, 564, 1–38.

4. Kaiser, C.; Hallbritter, T.; Heckel A.; Wachtveil, J. Thermal, Photochromic and Dynamic Properties of Water-Soluble Spiropyrans, ChemistrySelect, 2017, 2, 4111-4123.

5. Tsuruoka, T.; Hayakawa, R.; Kobashi, K.; Higashigushi, K.; Matsuda K.; Wakayama, Y. Laser Patterning of Optically Reconfigurable Transistor Channels in a Photochromic Diarylethene Layer, Nano Lett., 2016, 16, 7474-7480.

6. Wu, L.Y.L.; Zhao, Q.; Huang, H.; Lim, R.J. Sol-Gel Based Photochromic Coating for Solar Responsive Smart Window, Surf. Coat. Technol., 2017, 320, 601-607.

7. Fleisch, T.H.; Mains, G.J. An XPS Study of the UV Reduction and Photochromism of MoO_3 and WO_3, J. Chem. Phys., 1982, 76, 780–786.

8. Zong, Y.H.; Zhao, J.Z.; Zhao Y.; Huang, Z.F. Aqueous Synthesis and Photochromic Study of Mo/W Oxide Hollow Microspheres, RSC adv., 2016, 6, 99898-99904.

9. Besnadadiere, J. ; Ma, B. ; Torres-Pardo, A. ; Wallez, G. ; Kabbour, H. ; Gonzalez-Calbet, J.M. ; Von Bardeleben, H.J. ; Fleury, B. ; Buissette, V. ; Sanchez, C. ; Le Mercier, T. ; Cassaignon S. ; Portehault, D. Structure and Electrochromism of Two-Dimensional Octahedral Molecular Sieve h'-WO_3, Nature Com., 2019, 10, 327-330.

10. Zhang, Y.Z.; Huang, Y.S.; Cao, Y.Z.; Kuai, S.L.; Hu, X.F. Photochromism of Molybdenum Trioxide Sol and Gel, Acta Chim. Sin., 2001, 59, 2076-2079.

11. Granqvist, C.G. Handbook of Inorganic Electrochromic Materials, Elsevier, 1995.

12. He T.; Yao, J.N. Photochromism in Transition-Metal Oxides, Res. Chem. Intermed., 2004, 30, 459-488.

13. Wei, J.; Jiao, X.L.; Wang T.; Chen, D.R. Electrospun Photochromic Hybrid Membranes for Flexible Rewritable Media, ACS Appl. Mater. Interfaces, 2016, 8, 29713-29720.

14. Wang, S.L.; Kershaw, S.V.; Li G.S.; Leung, M.K.H. The Self-Assembly Synthesis of Tungsten Oxide Quantum Dots with Enhanced Optical Properties, J. Mater. Chem. C, 2015, 3, 3280-3285.

15. Wei, J.; Jiao, X.L.; Wang T.; Chen, D.R. The fast and Reversible Intrinsic Photochromic Response of Hydrated Tungsten Oxide Nanosheets, J. Mater. Chem. C, 2015, 3, 7597-7603.

16. Alcober, C.; Alvarez, F.; Bilmes S.A.; Candal, R.J. Photochromic W-TiO_2 Membranes, J. Mater. Sci. Lett. 2002, 21, 501-504.

17. Liu, S.; Fu, S.; Zhang, X.; Wang, X.; Kang, L.; Chen, X.; Wu J.; Liu, Y. Enhancing Hologram Memory via Deposition of Plasmonic Nanocubes on Orderly Mesoporous Titania, Optical Mater. Express, 2018, 8, 1143-1153.

18. Sol C.; Tilley, R.J.D. Ultraviolet Laser Irradiation Induced Chemical Reactions of some Metal Oxides, J. Mater. Chem., 2001, 11, 815-820.

19. Pan, L.; Wang, Y.; Wang, X.J.; Qu, H.Y.; Zhao, J.P.; Li Y.; Gavrilyuk, A. Hydrogen Photochromism in Nb_2O_5 Powders, Phys. Chem. Chem. Phys., 2014, 16, 20828-20833.

20. Deb S.K.; Chopoorian, J.A. Optical Properties and Color-Center Formation in Thin Films of Molybdenum Trioxide, J. Appl. Phys. 1966, 37, 4818-4825.

21. He T.; Yao, J.N. Photochromic Materials Based on Tungsten Oxide, J. Mater. Chem., 2007, 17, 4547-4557.

22. He, T.; Ma, Y.; Cao, Y.A.; Jiang, P.; Zhang, X.; Yang W.S; Yao, J.N. Enhancement Effect of Gold Nanoparticles on the UV-Light Photochromism of Molybdenum Trioxide Thin Films, Langmuir, 2001, 17, 8024-8027.

23. Yao J.N.; Loo, B.H. Improved Visible-Light Photochromism in Au/MoO_3 SnO_2 Thin Films, Solid State Com. 1998, 105, 479-480.

24. Yao, J.N.; Yang Y.A.; Loo, B.H. Enhancement of Photochromism and Electrochromism in MoO_3/Au and MoO_3/Pt Thin Films, J. Phys. Chem. B, 1998, 102, 856-1860.

25. He, T.; Cao, Y.A.; Yang W.S.; Yao, J.N. Improved Photochromism of WO_3 Thin Films by Addition of Au Nanoparticles Phys. Chem. Chem. Phys K. 2002, 4, 1637-1639.

26. Fox M.A.; Dulay, M.T. Heterogeneous Photocatalysis, Chem. Rev. 1993, 93, 341-357.

27. Linsebigler, A.L.; Lu, G.; Yates, J.T. Photocatalysis on TiO_2 Surfaces: Principles, Mechanisms, and Selected Results, Chem. Rev. 1995, 95, 735-758.

28. Quevedo-Lopez, M.A.; Reidy, R.F.; Orozco-Teran, R.A.; Mendoza-Gonzalez, O.; Ramirez-Bon, R. Enhancement of the Photochromic and Thermochromic Properties of Molybdenum Oxide Thin Films by a Cadmium Sulfide Underlayer, J. Mater. Sci. Electronics, 2000, 11, 151-155.

29. Zhao, Z.G.; Liu Z.F.; Miyauchi, M. Tailored Remote Photochromic Coloration of in situ Synthesized CdS Quantum Dot Loaded WO_3 Films, Adv. Funct. Mater. 2010, 20, 4162-4167.

30. Faughman B.W.; Crandall, R.S. Optical Properties of Mixed-Oxide WO_3/MoO_3 Electrochromic Films, Appl. Phys. Lett., 1977, 21, 834-836.

31. Yao, J.N.; Loo, B.H.; Kashimoto K.; Fujishima, F. Photochromic Characteristics of Mixed WO_3–MoO_3 Thin Films in Alcohol Vapors, Ber. Bunsen- Ges. Phys. Chem., 1991, 95, 554-556.

32. Ahmed H.M.F.; Begum, N.S. Synthesis and Characterization of MoO_3–WO_3 Composite Thin Films by Liquid Phase Deposi-

tion Technique: Investigation of its Photochromic Properties, Bull. Mater. Sci. 2013, 36, 45-49.

33. Liu, Y.; He, H.Z.; Li, J.; Li, W.Z.; Yang, Y.H.; Li Y.M.; Chen, Q.Y. ZnO Nanoparticle-Functionalized WO_3 Plates with Enhanced Photoelectrochemical Properties, RSC Adv. 2015, 5, 46928-46934.

34. He, T.; Ma, Y.; Cao, Y.A.; Liu, H.M.; Yang W.S.; Yao, J.N. Comparison between the Effects of TiO_2 Synthesized by Photoassisted and Conventional Sol–Gel Methods on the Photochromism of WO_3 Colloids, J. Colloid Interface Sci. 2004, 279, 117-123.

35. Song, Y.Y.; Gao, Z.D.; Wang, J.H.; Xia X.H.; Lynch, R. Multistage Coloring Electrochromic Device Based on TiO_2 Nanotube Arrays Modified with WO_3 Nanoparticles, Funct. Mater. 2011, 21, 1941-1946.

36. Palgrave R.G.; Parkin, I.P. Aerosol Assisted Chemical Vapour Deposition of Photochromic Tungsten Oxide and Doped Tungsten Oxide Thin Films, J. Mater. Chem., 2004, 14, 2864-2867.

37. Yang, H.; Li X.; Wang, A.; Wang, Y.; Chen, Y. Photocatalytic Degradation of Methylene Blue by MoO_3 Modified TiO_2 under Visible Light, Chin. J. Catal., 2014, 35, 140-147.

38. Elder, S.H.; Cot, F.M.; Su, Y.; Heald, S.M.; Tyryshkin, A.M.; Bowman, M.K.; Gao, Y.; Joly, A.G.; Balmer, M.L.; Kolwaite, A.C.; Magrini K.A.; Blake, D.M. The Discovery and Study of Nanocrystalline TiO_2-(MoO_3) Core–Shell Materials, J. am. Chem. Soc., 2000, 122, 5138-5146.

39. Li, N.; Cao, X.; Chang, T.; Long S.; Jin, P. Selective Photochromism in a Self-Coated WO_3/WO_{3-x} Homojunction: Enhanced Solar Modulation Efficiency, High Luminous Transmittance and Fast Self-Bleaching Rate, Nanotechnol., 2019, 30, 25570-25580.

40. https://www.pveducation.org/pvcdrom/properties-of-sunlight/average-solar-radiation.

41. Serier, H.; Gaudon M.; Ménétrier, M. Al-doped ZnO Powdered Materials: Al Solubility Limit and IR Absorption Properties, Solid State Sciences, 2009, 11, 1192-1197.

42. Al-Gaashani, R.; Radiman, S.; Daud, A.R.; , N.Tabet, N.; Al-Douri, Y. XPS and Optical Studies of Different Morphologies of ZnO Nanostructures Prepared by Microwave Methods, Ceramics International, 2013, 39, 2283–2292.

43. Muchuweni, E.; Sathiaraj, T.S.; Masanganise, J.; Muchanyereyi, N. The Effect of RF Power on the Properties of Gallium and Aluminium Co-Doped Zinc Oxide (GAZO) Thin Films, Journal of Inorganic and Organometallic Polymers and Materials, 2019, 29, 49–58.

44. Peng, Y.-Y; Hsieh, T.-S.; Hsu, C.-H. White-Light Emitting ZnO–SiO_2 Nanocomposite Thin Films Prepared by the Target-Attached Sputtering Method, Nanotechnology, 2006,17, 174–180.

45. Trenque, I.; Mornet, S.; Duguet E.; Gaudon, M. Establishment of the Correlation Law between Electron Density, Infrared Absorption and Doping Concentration in Ga^{3+}-Doped ZnO, Mater. Res. Bull., 2013, 48, 1155-1159

46. Zhang, J.G.; Benson, D.K.; Tracy, C.E.; Webb J.; Deb, S.K. Self-bleaching mechanism of electrochromic WO_3 films, Proc. Optical materials technology for Energy Efficiency and Solar Energy Conversion XII, 1993, 104-112.

47. Wang M.; Koski, K.J. Reversible Chemochromic MoO_3 Nanoribbons through Zerovalent Metal Intercalation, ACS nano, 2015, 9, 3226-3233.

48. Bamfield, P.; Hutchings, M. Chromic Phenomena: Technological Applications of Colour Chemistry, 2nd Edition: Royal Society of Chemistry, 2010 – Science.

TOC Graphic

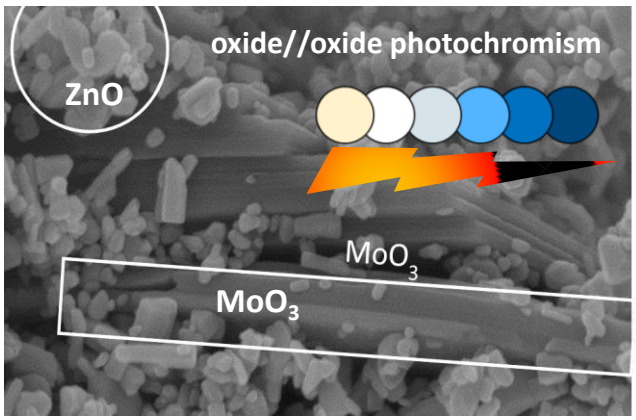
ZnO
oxide//oxide photochromism
MoO3
MoO3

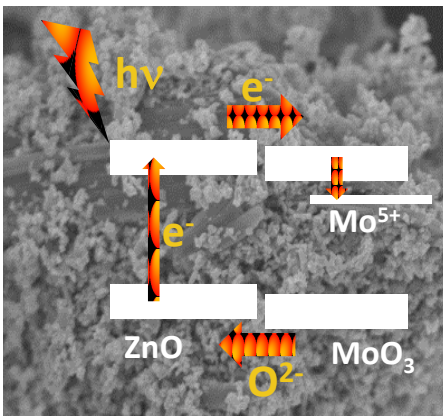
hν
e-
e-
Mo5+
ZnO
O2-
MoO3